# Broad spectrum compounds targeting early stages of rabies virus (RABV) infection

Sabrina Kali, Corinne Jallet, Saliha Azebi, Thomas Cokelaer, Juliana Pipoli da Fonseca, Yu Wu, Julien Barbier, Jean-Christophe Cintrat, Daniel Gillet, Noël Tordo

Version of Record: https://www.sciencedirect.com/science/article/pii/S0166354221000061
Manuscript_c8f9a45d8bd6dee9fcea82c379e9b000

# Broad spectrum compounds targeting early stages of RABV infection

Sabrina Kali [a,b], Corinne Jallet [a], Saliha Azebi [a,c,d], Thomas Cokelaer [c,e], Juliana Pipoli Da Fonseca [c], Yu Wu [f], Julien Barbier [f], Jean-Christophe Cintrat [g], Daniel Gillet [f], Noël Tordo [a,h]

[a] Unit Antiviral Strategies, Institut Pasteur, 75724, Paris, France
[b] Institut Pasteur d'Algérie, Dely Ibrahim, Alger, Algeria
[c] Plate-forme Technologique Biomics – Centre de Ressources et Recherches Technologiques (C2RT), Institut Pasteur, 75724, Paris, France
[d] Unit Viral Neuroimmunology, Institut Pasteur, 75724, Paris, France
[e] Hub de Bioinformatique et Biostatistique, Institut Pasteur, USR 3756 CNRS, 75724, Paris, France
[f] Service d'Ingénierie Moléculaire des Protéines (SIMOPRO), CEA, Université Paris-Saclay, 91191, Gif-sur-Yvette, France
[g] Service de Chimie Bioorganique et Marquage (SCBM), CEA, Université Paris-Saclay, 91191, Gif-sur-Yvette, France
[h] Institut Pasteur de Guinée, BP 4416, Conakry, Guinea

Corresponding authors : Noël TORDO, Unit Antiviral Strategies, Institut Pasteur, 25 rue du Dr. Roux, 75724 Paris Cedex 15 France, <ntordo@pasteur.fr>

Keywords : rabies virus, endosomal pathway inhibitors, drug synergy, late endosome, rabies glycoprotein.

## Abstract (219 words)

ABMA and its analogue DABMA are two molecules of the adamantane family known to perturbate the endosomal pathway and to inhibit cell infection by several RNA and DNA viruses. Their activity against Rabies Virus (RABV) infection *in vitro* has already been demonstrated *in vitro*. (Wu et al., 2017, 2019). Here, we describe in more details their mechanism of action by comparison to Arbidol (umifenovir) and Ribavirin, two broad spectrum antivirals against emerging viruses such as Lassa, Ebola, influenza and Hantaan viruses. ABMA and DABMA, delivered 2 h pre-infection, inhibit RABV infection *in vitro* with an $EC_{50}$ of 7.8 µM and 14 µM, respectively. They act at post-entry, by provoking RABV accumulation within the endosomal compartment and DABMA specifically diminishes the

expression of the GTPase Rab7a controlling the fusion of early endosomes to late endosomes or lysosomes. This may suggest that ABMA and DABMA act at different stages of the late endosomal pathway as supported by their different profile of synergy/antagonism with the fusion inhibitor Arbidol. This difference is further confirmed by the RABV mutants induced by successive passages under increasing selective pressure showing a particular involvement of the viral G protein in the DABMA inhibition while ABMA inhibition induces less mutations dispersed in the M, G and L viral proteins. These results suggest new therapeutic perspectives against rabies.

# 1. Introduction (453 words)

The etiologic agent of rabies disease belongs to the *Lyssavirus* genus, *Rhabdoviridae* family (www.ictv.global/report/rhabdoviridae). Although preventable preventable by vaccination pre- or post-exposure (WHO, 2020), rabies still provokes about 59,000 human deaths and 8.6 billion USD economic losses per year (Hampson et al., 2015). Considering the long incubation period of rabies (2 months in human), the antiviral approach is a promising alternative. Over the last 30 years compounds proven active against other pathogens have shown some anti-RABV effect *in vitro*, rarely confirmed *in vivo* (Castel et al, 2015). For example IFN-α (Postic and Fenje, 1971), dermaseptins inhibiting viral entry (Mechlia et al., 2019), amantadine and chloroquine blocking pH dependent endosomomal pathway (Superti et al., 1985; Tsiang and Superti, 1984) or molecules acting on viral replication such as Favipiravir (Banyard et al., 2019) or nucleoside analogues broadly active on RNA viruses such as VSV and RSV (Jochmans and Neyts, 2019). The FDA approved drugs repurposing strategy could be a good alternative to fight rabies in combination therapy. This was the philosophy of the Milwaukee protocol (Willoughby et al., 2005) applied in 2005 to a symptomatic teenager previously bitten by a bat. This empirical treatment combined benzodiazepine with drugs having shown *in vitro* anti-RABV effect, i.e. Ketamine (Tsiang et al., 1991), Ribavirin (Bussereau et al., 1983), and Amantadine (Superti et al., 1985). Although the teenager recovered, this protocol mostly failed with other symptomatic patients (Aramburo et al., 2011; Hemachudha et al., 2006; Manesh et al., 2018) leading to a controverse around its scientific basis (Jackson, 2013) . Besides this controverse, this protocol has opened a new perspective in antiviral research for a neglected disease like rabies

ABMA and its analogue DABMA are two drugs known to perturbate the endosomal pathway and inhibit several RNA and DNA viruses including RABV (Wu et al., 2017; Wu et al.,

2019). In the present work, we focus on determining their mechanism of action on RABV infection *in vitro* by comparing their activity to that of Arbidol (*umifenovir*) (Haviernik et al., 2018) and Ribavirin, two broad spectrum antivirals. Ribavirin, a synthetic guanosine nucleoside which depletes intra-cellular GTP, interferes with viral mRNA synthesis (Moriyama et al., 2008) and inhibits the polymerase activity as exemplified for hepatitis E (Debing et al., 2014) and hepatitis C (HCV) viruses (Paeshuyse et al., 2011). It is used to treat HCV, Respiratory Syncitial virus (RSV) and Lassa fever virus (LASV) (Hadi et al., 2010). Arbidol, first marketed in 1993 in Russia for treatment of influenza virus A and B, is a viral fusion inhibitor (Boriskin et al., 2008) efficient against several viruses (Delogu et al., 2011) including Ebola virus *in vitro* (Pecheur et al., 2016) and Hantaan virus *in vitro* and *in vivo* (Deng et al., 2009).

## 2. Material and methods (1543 words)

### 2.1 Cell lines, rabies virus and antibodies

BSR cells (clone of BHK-21) were maintained in Dulbecco's Modified Eagle Medium (DMEM) with 8% Fetal Bovine Serum (FBS), gentamycin 40 µg/ml, 5% CO2 in 96 well plates. BHK-T7 were maintained in MEM-Glasgow with 10% FBS supplemented with 4% Tryptose Phosphate Broth (TPB) and Pennicillin (100U/ml) / Streptomycin (100µg/ml). The Pasteur Virus (PV) strain of RABV was used for infection experiments.

The following anti-RABV antibodies have been used: a mouse monoclonal antibody (MAb) anti-N conjugated with FITC (Fudjerebio); a rabbit polyclonal antibody (PolAb) anti-RNP and a mouse MAb anti-G protein (D1), both produced in the laboratory (Tuffereau et al., 2001; Fournier et al., 2003); a mouse MAb anti-M protein kindly provided by S. Finke (Friedrich Loeffler Institute, Griefswald, Germany). A mouse MAb anti-calnexin, a mouse MAb anti-tubulin, a rabbit PolAb anti-Rab7a, an anti-rabbit goat antibody and an anti-mouse goat antibody were purchased (Sigma).

### 2.2 Compounds

The molecule ABMA (1-adamantyl (5-bromo-2-methoxybenzyl) amine) was initially selected by a cell-based high-throughput screening assay as a ricin and shiga-like toxin inhibitor blocking the retrograde trafficking at the endosome-TGN interface (Stechmann et al., 2010). Its inhibitory effect on the endosomal pathway further extended to other pathogens including bacteria, parasites and viruses such as RABV (Wu et al, 2017). Several ABMA derivatives were screened for their activity against RABV infection *in vitro* (data not shown) and DABMA (1-dimethyl-ABMA) was selected (Wu et al, 2019). ABMA and DABMA compared in the present study were provided by the Centre d'Energie Atomique (Gif-sur-Yvette), their structure in available in Supplementary data 1. Arbidol (ethyl-6-bromo-4-

[(dimethylamino)methyl]-5-hydroxy-1-methyl-2[(phenylthio)methyl]-indole-3-carboxylate hydrochloride monohydrate), Ribavirin (1-β-D-Ribofuranosyl-1,2,4-triazole-3-carboxamide), EGA (2-[(4-Bromophenyl)methylene]-N-(2,6-dimethylphenyl)-hydrazinecarboxamide) and Cycloheximide (3-[2-(3,5-Dimethyl-2-oxocyclohexyl)-2-hydroxyethyl]glutarimide), were purchased from Sigma. Stock solutions in 30 mM of dimethyl sulfoxide (DMSO) were conserved at -20°C. To calculate the selectivity index of each drug, the cytotoxicity of the compounds for 24h on BSR cells was evaluated using Cell Titer-Glo Luminescent Cell Viability Assay (Promega). This experiment was repeated twice, with each point in quadriplicate.

**2.3 Pre-infection and post-infection protocol for compounds delivery**

BSR cells (35000 cells/well) were incubated in DMEM 8% FBS, gentamycin 40 µg/ml for 24h at 37°C in 96 well plates. For pre-infection protocol, the medium was removed and cells were pre-incubated for 2h at 37°C in DMEM 2% FBS, gentamycin 40µg/ml in presence of compounds at 1 to 30 µM. RABV (MOI=20) was then added for 1h, the cells were washed with DMEM to remove the residual RABV, then incubated for 24h at 37°C in DMEM 2% FBS, gentamycin 40 µg/ml in presence of the compounds at the initial concentration. For post-infection protocol, the cells were first infected with RABV (MOI=20) in DMEM 2% SVF, gentamycin 40µg/ml for 2h at 37°C, washed with DMEM, then incubation continued for 24h while various concentration of the compounds were added after the 2 first hours.

The percentage of infected cells showing intracellular replication of RABV was evaluated as previously described (Mechlia et al., 2019). Briefly the cells were washed with Phosphate Buffered Saline (PBS) Ca++, Mg++, then fixed with acetone 80% during 20 min at 4°C. A mouse MAb anti-N conjugated with FITC (Fudjerebio) diluted 1/200 in PBS was incubated for 1h at 37°C to detect the cytoplasmic inclusions of RABV RNP (Negri bodies). Nucleus

staining was performed by dilution of Hoechst (33342) 1/2000 in PBS. Images were acquired on an automated spinning disk confocal microscope (Opera QEHS, Perkin Elmer Technologies) at the Imagopole (Institut Pasteur imaging platform). Results were averaged from at least two independent experiments, each point being performed in quadriplicate.

To evaluate the RABV released by the infected/treated cells, the supernatants were diluted 1/100 to 1/2700 in DMEM 10% FBS, gentamicin 40 µg/ml, titrated immediately or frozen for later analysis. Titer was evaluated in plaque forming units per mL (PFU/mL) on fresh BSR cells. The experiment was repeated twice, each point was perfomed in duplicates.

**2.4 Evaluation of RABV transcription/replication using the minireplicon assay**

The minireplicon assay recreating a RABV RNP complex active in transcription and replication was modified from (Castel et al., 2009). The plasmid pBl DI encoding a RABV minigenome expressing luciferase and the plasmids pTM1-N, pTM1-P, pTM1-L encoding the corresponding RABV proteins are placed under the control of the T7 RNA polymerase promoter. Each well of 96 well plate of BHK-T7 cells stably expressing the T7 RNA polymerase was seeded (35.000 cells / well) in 100 µl of MEM-TPB, 2 mM glutamine + 5% FBS, gentamycin 40 µg/ml in the presence of 20µM of the tested compounds. After 24h at 37°C, the supernatant was removed and the BHK-T7 cells were transfected with 50 µl containing plasmids pTM1-N (0.1 µg), pTM1-P (0.1 µg), pTM1-L (0.02 µg), pBl DI (0.05 µg) and 3 µl of FuGENE / µg of DNA previously incubated for 15 min at room temperature simultaneously with 50 µl of compounds at a final concentration of 20 µM. After 48h the medium was removed and the luciferase produced was evalated in arbitrary unit (RLU) as described in (Castel et al., 2009). The mean value was calculated from two independent experiments, each point in quadriplicate.

**2.5 qPCR experiments**

Total RNA present in cell supernatant of infected BSR cells was extracted using the QiAmp Viral RNA mini kit (Qiagen). Cell lysates were treated with the "DNA RNA and protein purification kit" (Macherey-Nagel). All extractions were treated with DNAse using the Turbo DNA-free kit (Themo Fisher). To specifically quantify the genome (- strand) of RABV the reverse transcription using Superscript III RT was initiated with a forward (+) sense primer (F) started at genomic position 1 (leader gene). The cDNA was then amplified between this F primer and a reverse primer (R) in the N gene providing a 165 nucleotide long amplicon (Supplementary data 2). The qPCR used SYBRgreen on an ABI PRISM 7500 Fast Real-Time Machine (Applied Biosystems). The experiment was performed two times with two replicates for each condition.

**2.6 Following M and G proteins at early stages of RABV infection**

BSR cells were cultivated in µ-Slide 8 wells in DMEM 2% FBS, 40µg/µl gentamycin for 24h at 37°C. For profiling the M protein, 10µg/ml cycloheximide were added for 30 min in presence of 60µM ABMA, or 40µM DABMA, or 40µM EGA. Then cells were infected with RABV PV strain (MOI= 500) for 2h at 37°C, washed with DMEM, readjusted with ABMA, DABMA or EGA compounds at their initial concentrations in DMEM 2% FBS, 40µg/µl gentamycin and incubated for 4h or 9h at 37°C. The cells were fixed for 10 min with PFA 4% then permeabilized for 10 min with TritonX100 0,1% with washing with PBS 1% / BSA 0,1 % after each step. Cells were incubated for 1h at room temperature with an anti-M RABV mouse Mab, further revealed by a secondary anti-mouse antibody conjugated to Alexa488. Nuclei were stained with Hoechst (Invitrogen) diluted at 1/2000.

To follow the G and Rab7a proteins, two primary antibodies were used : a mouse MAb anti RABV-G protein (D1, 1/1000); a rabbit PolAb anti-Rab7a (1/300). The labelling was

performed with an anti-rabbit secondary Mab tagged with Alexa555 (1/2000) and an anti-mouse Mab tagged with Alexa488 (1/500).

### 2.7 Next generation sequencing of resistant mutants to the compounds (PacBio methodology)

BSR cells were infected with the PV strain RABV (MOI=20) following the 2h pre-infection protocol. 16 passages were performed with increasing concentrations of ABMA, DABMA or Ribavirin from 5 µM then 6, 8, 10, 12, 13, 14, 15, 17, 18, 19, 20, 21 up to 22 µM. Two passages were performed at 13 and 14 µM. For each passage the incubation time was 72h. 75 µL from the supernatants produced were used as inoculum for the next passage, the rest was stored at -80°C for further analysis.

The RNA was extracted from 140 µL of clarified supernatants (Nucleospin kit, Qiagen) and reverse transcribed with random hexamers (Transcriptor First Strand cDNA Synthesis kit, Roche). The RABV genome cDNA was specifically amplified in 6 overlapping cDNA fragments (Supplementary data 2) using the "Expand High Fidelity PCR System" kit (Roche). The 6 fragments from each sample were equimolarily pooled, barcoded , loaded on one SMRTcell and sequenced using the 2.1 Pacific Biosciences chemistry and 20h movie format on Sequel I system.

The Pacbio data was first analysed within the SMRT Link v5.1 software. The raw reads were demultiplexed, and the quality filtered reads were selected and processed to obtain circular consensus sequences (CCS) with at least 100 bases, 5 complete passes and a minimum accuracy of 0.99. CCS reads were mapped onto the reference RABV genome using the Sequana framework (Eduati et al., 2017). A dedicated Pacbio amplicon analysis pipeline (v 0.8.0) further analyse the CCS reads for contaminants and single nucleotide polymorphism (SNPs) using freebayes software (https://arxiv.org/abs/1207.3907).

### 2.8 Drug combination assay

Pairwise combinations of various concentration (1µM to 30µM) of ABMA, DABMA and Arbidol were performed using the pre-infection protocol. The inhibition potential of each combination on the intracellular replication of RABV RNP in BSR cells was evaluated as described before. The synergistic or antagonistic effect of the different combinations was assessed according to two mathematical models of interaction: the Bliss independence model and the Lowe additivity model (Bliss, 1939; Loewe, 1953). Each experimental point was tested in quadriplicate in at least two independent experiments and the average value was calculated.

# 3. Results (1725 words)

### 3.1 Effect of ABMA, DABMA and arbibol on RABV infection using pre- or post-infection protocols

Previous works have reported the potential of the ABMA compound and its derivative DABMA to protect cells against various toxins, parasites, intracellular bacteria and viruses sharing a pH-dependent mechanism for cytoplasmic penetration (Dai et al., 2018; Wu et al., 2017; Wu et al., 2019). In order to further explore the basic mechanism of this inhibition, we compared the anti-RABV effect of ABMA to that of DABMA and of the fusion inhibitor Arbidol. The inhibitory effect was assessed 24 h after infection of BSR cells with the RABV PV strain by counting the infected cells (Negri bodies in the cytoplasm). We compared adding the drugs 2h before infection, to just after removing the RABV inoculum. In pre-infection protocol, the three compounds showed a dose dependent inhibitory effect from 10 µM to 30 µM: DABMA had an improved inhibitory capacity compared to ABMA visible both through the number of infected cells (Fig. 1A) and with the amount of intra-cytoplasmic RABV RNP (Supplementary data 3). Arbidol displayed an intermediate effect in between DABMA and ABMA (Fig. 1A). Inhibition was clearly lower using the post-infection protocol : at 10 µM no real difference appeared between the compounds; at 20 µM and 30 µM DABMA showed 50% inhibition followed by Arbidol while ABMA did not show any substantial inhibition (Fig. 1B).

The IC50s confirmed the decreased inhibitory performance from DABMA (7.8 µM and 14 µM in pre- and post-infection, resp.) to Arbidol (8.5 µM and >30 µM, resp.) down to ABMA (22.5 µM and >30 µM, resp.) (Table 1). The Selectivity Index (SI) was calculated after evaluation of the cytotoxicity of each compounds for BSR cells using the “Cell Titer-Glo Luminescent Cell Viability Assay” (Promega) (data not shown). The SI matched the IC50

gradation, i.e. DABMA SI (5.4) was slighly to largely better than that of Arbidol (6.9) and ABMA (>7.5), respectively (Table 1).

The inhibitory effect of the compounds was further assessed by titration of the neo-RABV produced in the treated cell-supernatant on fresh BSR cells. Figure 1C shows the results of the most-effective pre-infection protocol. We observed the same trends: DABMA and Arbidol decreased the RABV release of about 1 log at 10 µM and almost completely at 20 µM; ABMA was at least 1 log less efficient. Figure 1D shows that the decrease in RABV genomic RNA in the supernatants, quantified by qPCR, roughly paralleled the decrease of infection rate confirming that the inhibitory effect was really due to the decrease in RABV release and not to the unability of the RABV progeny to infect fresh BSR cells.

### 3.2 Effect of ABMA, DABMA or Ribavirin on the RABV minireplicon system

The better inhibitory effect of ABMA, DABMA in the pre-infection protocol, similarly to the fusion inhibitor Arbidol, suggests that they act at early stages of RABV infection. To clarify this point, we compared the effect of 20 µM of ABMA and DABMA with that of Ribavirin, a nucleoside analogue, on a RABV minireplicon competent in transcription and replication. After 48 h, the activity of the minireplicon was measured by quantifying the luciferase signal. Ribavirin clearly inhibited 80% of the luciferase activity compared to untreated BHK-T7 cells (Fig. 2). In contrast the inhibitory effect of ABMA was null (even 20% more luciferase signal than control) and that of DABMA only very limited (25% inhibition). These results confirmed that ABMA and DABMA act before the genome transcription/replication, somewhere between entry and post-entry of the RABV into the cell.

### 3.3 Effect of ABMA and DABMA on early steps of RABV infection

To better understand at which post-entry step AMBA and DABMA exert their inhibition, BSR cells were treated with cycloheximide to block viral and cellular translation, then infected with the RABV PV strain at a very high MOI (500) to vizualize the viral input in the presence of ABMA (40 µM), DABMA (40 µM) or EGA (40 µM), a compound known to inhibit the traffic from early endosomes to more acid compartments (Gillespie et al., 2013). The entry of RABV particules into the cells was monitored during 4 h and 9 h using a anti-M protein MAb (Fig. 3A). In the absence of compound, the M protein was observed 4 h post-infection as green points which disappeared 9 h post-infection, signing a progressive penetration into downstream endosomal compartments or dilution into the cytosol or degradation into lysomes. In contrast, in presence of ABMA, DABMA or EGA, the accumulation of M protein persisted and even increased in number and size 9 h post-infection. A quantification of RABV M protein inclusions in 5 fields of 100 cells was performed at 9 h post-infection. About 20-25% of cells treated with ABMA, DABMA or EGA still showed M protein accumulation compared to 2% in control cells (Fig 3B). This result indicates that ABMA, DABMA and EGA compounds block the viral input into the endosomal pathway.

EGA has been shown to block the anthrax lethal toxin by inhibiting trafficking in acidified endosomes, without affecting endosome pH (Gillepsie et al., 2013), at an early step of the endosomal pathway (Wu et al., 2020). To precise the step targetted by ABMA and DABMA, we measured their capacity to interfere with the expression of two markers of the endosomal pathway: the EEA1 protein which is specific of early endosome and interacts with the GTPase Rab5a; the GTPase Rab7a known to be involved downstream, in the fusion of early endosomes with late endosomes or lysosomes. Using immunofluorence, both EEA1 and Rab7a appeared as cytoplasmic red dots in cells (Fig. 3C). As expected, both ABMA (60µM) and particularly DABMA (30µM) provoked a clear decrease in the amount of RABV

glycoprotein staining. However none of them inhibited EEA1 expression. Interestingly, 60µM ABMA had no major effect on Rab7a amounts or localization in cells while only 40µM DABMA, clearly inhibited Rab7a (Fig 3C). We confirmed by quantitative PCR that 30µM DABMA inhibited 50% of the Rab7a mRNA expression while 60µM ABMA inhibited only 20% (Fig. 3D). The same observation was done by Western blott (Supplementary data 4). Interestingly, the expression of Rab5a mRNA, a protein interacting with EEA1 in early endosomes, was not affected (data not shown). This result suggests that DABMA and less efficiently ABMA, are acting downstream in the late endosomal pathway.

**3.4 Synergistic effects of drug combinations**

To investigate if ABMA, DABMA, and Arbidol have an additive or synergistic effect on inhibition of RABV infection, the 3 possible 2-drug combinations (ABMA/DABMA, ABMA/Arbidol, DABMA/Arbidol) were tested at 7 concentrations from 1 µM to 30 µM (i.e. 49 combinations). The Bliss independence model and the Lowe additivity model were used (Hampson et al., 2015; He et al., 2018) and the software Combenefit calculated the scores of synergy. Both models giving similar scores, only the results of the Bliss model are presented (Fig. 4A) under a matrix format and a three dimentional presentation outlining the synergetic (positive in blue) or antagonistic (negative in red) effects of each combination (Di Veroli et al., 2016). The combination ABMA/DABMA showed a high synergy with the compounds at low concentrations. For example the combination DABMA 10 µM / ABMA 1 µM gave 90 % of inhibition (synergy score +23) while DABMA 10 µM showed only 50% inhibition and ABMA 1 µM (IC50 = 19.8 µM) had virtually no effect (Fig 4B). However at high concentration, ABMA appeared antagonistic with DABMA, possibly due to the cytotoxicity of the combined compounds. Interestingly, in combination with Arbidol, ABMA dispayed a similar synergistic/antagonist profile and scores than with DABMA : at low concentrations (1

and 5 µM) ABMA is synergistic with all the concentrations of Arbidol. For example, the combination Arbidol 10 µM / ABMA 1 µM induced 80 % of inhibition, a better value than the indidual drugs at the same concentrations (Fig. 4B). Finally, the DABMA / Arbidol combinations were the less synergistic for RABV inhibition with a symetry of antagonism between the highest concentrations of one compounds and the lower of the other.

### 3.5 Selection of mutants resistant to ABMA, DABMA and Ribavirin

To explore possible viral adaptation to ABMA, DABMA and Ribavirin treatments, we passaged the RABV PV strain on BSR cells for 16 consecutive passages of 72 h each, increasing progressively the compound concentration from 5 µM to 22 µM. The supernatant of each passage was used to infect the cells of the following one (Fig 5A). Then, the full length genome was sequenced through 6 amplicons (PacBio technology) with a depth of 8000 to 26000 sequences (mean 14500) per nucleotide allowing a precise analysis of single nucleotide polymorphism (SNPs).

Interestingly, the RABV PV Strain used in the experiment had significantly evolved compared to that published in Genbank (Tordo et al., 1986 ; Tordo et al., 1988) (ACCESSION NC_001542) with 14 nucleotide mutations (11 changes, 2 insertions, 1 deletion) resulting in 6 amino acid changes in the Glycoprotein and the Polymerase (Table 2). Following the 16 passages in absence of compound, only 3 synonymous nucleotide changes were observed in about 25% of the genome population (Table 2). The situation was similar after 16 passages with increasing amounts of Ribavirin: only 4 nucleotide changes in 15-25% of the genome population with only 1 non synonymous in the Polymerase (S1128L). After 16 passages with increasing concentrations of ABMA, the number of nucleotide changes was similar (5) but 4 of them were non synomymous in the Matrix (L43Q), Glycoprotein (183V) and Polymerase (S113I; N169D) some of them becoming dominant in the genome population

(50-70%). Finally, the 16 passages with increasing concentrations of DABMA were the most mutagenic, provoking 10 nucleotide changes among which 6 were non synonymous : 1 in the Matrix (D147L) and 5 in the Glycoprotein (V48G; V152A; D209N; A213L; G247E) in variable proportion of the genome population (25 to 50%). This observation suggests a particular involvement of the G protein in the inhibition mechanism of DABMA.

We compared the supernatant of the $16^{th}$ passage to the initial RABV PV strain. Both viral population were used at the same MOI = 10, using the 2h pre-infection protocol in BSR cells described above, with 30µM of DABMA, a concentration superior to that of the $16^{th}$ passage. While DABMA treatment fully inhibited the infection of the original RABV (100% inhibition), only 30% inhibition was observed for the $16^{th}$ passage mutant (data not shown).

## 4. Discussion (799 words)

Rabies is 100% fatal once the RABV has reached the nervous system and is no more accessible to antibodies elicited by vaccination (WHO, 2020). Searching for specific anti-RABV antivirals acting at this stage is unrealistic due to the gap existing between the cost for developing new drugs and the statute of neglected disease. It is more pragmatic to favour compounds with broad-spetrum activity, especially targeting cellular functions used by pathogens (Bekerman and Einav, 2015).Compounds targeting the endosomal pathway, such as amantadine that blocks the endosome acidification, are already used against influenza infections (Davies et al., 1965; Grunert et al., 1965). Adamantane derived compounds (Gerzon and Kau, 1967) with a lipophilic spherical cage of hydrocarbon amine have in addition the ability to naturally cross the blood brain barrier. They represent an interesting scaffold for treating diseases with neurological disorders (Crosby et al., 2003; Wanka et al., 2013).

Here, we describe the anti-RABV effect of two novel compounds sharing an adamantine skeleton: ABMA and its derivative DABMA. We show that DABMA given 2 h before infection is 3 times more effective than ABMA on RABV infection and slightly more effective than Arbidol, a viral fusion inhibitor of influenza virus (Boriskin et al., 2008), Ebola virus (Pecheur et al., 2016) and Hantaan virus (Deng et al., 2009). The inhibition potential of ABMA/DABMA is most probably acting post-entry, along the endosomal pathway, as supported by their similar effect with EGA and with the fusion inhibitor Arbidol. After binding of the RABV glycoprotein to its cellular receptors (Thoulouze et al., 1998) clathrin dependent vesicules are formed (Piccinotti et al., 2013). They fuse with early endosomes, then late endosomes and lysosomes. Acidification provokes a G protein conformational change resulting in the virus-endosome membrane fusion and the liberation of the ribonucleoprotein inside the cytoplasm. In A549 cells, ABMA and DABMA induce the accumulation of the

GTPase Rab7a that controls the fusion of early endosomes to late endosomes or lysosomes (Wu et al., 2020; Wu et al., 2017; Wu et al., 2019). In infected BHK-21 cells, we showed that the inhibitory effect of DABMA on RABV infection is accompanied by a decrease of Rab7a protein and RAB7A mRNA expression. This difference may depend on the cell type and/or on the pathogen, bacterial toxin and a neurotropic virus, respectively. As the expression of Rab5a mRNA, a marker of early endosomes, was not affected, this suggests that DABMA is acting downstream in the late endosomal pathway. ABMA did not show a decrease on Rab7a protein what may fit with its lower inhibitiory potential than DABMA or sign a slightly different mechanism for inhibition. This hypothesis is supported by the mutant selection process in presence of increased amounts of compounds. While Ribavirin and ABMA generated 1 and 4 non-synonymous changes respectively, dispersed along the RABV genome (M, G and L proteins), DABMA provoked 6 non-synonymous changes, 5 of them in the G protein. These mutations targetted particularly the central part of the ectodomain, between residues 150 and 250, which correspond to the conformational antigenic site II mostly exposed to the interaction with cellular components (Jallet et al., 1999; Prehaud et al., 1988). Using high throughput sequencing of long genomic fragments, it appeared that DABMA has selected two viral populations: the first one (50% of the population) associates the mutation D147L of the matrix with 2 mutations V152A, G247E of the glycoprotein. The second one (20% of the population) associates 2 synonymous changes in the matrix, with 3 mutations V48G, D209N, A213L of the glycoprotein. By analogy with VSV and the Mokola Virus (MOKV) G protein structure, the V48G mutation is located between the fusion domain (FD) and the pleckstrin homology domain (PHD) while the D209N and A213L mutations are embeded in the PHD, both domains being important in the conformation changes from the PRE- to the POST-fusion structure and for the receptor recognition. (Baquero et al., 2017; Belot et al., 2019)

These results suggest that the G protein is playing a specific role in the inhibition mechanism by DABMA. On the other hand, 2 non synonymous mutations obtained with ABMA target the M protein, the other viral partner involved in the endosomal pathway. The different inhibition mechanism of ABMA and DABMA is further supported by their scores of synergy when combined with Arbidol. ABMA shows high synergy at low concentration with both DABMA and Arbidol while DABMA and Arbidol are poorly synergetic, suggesting that they may compete on the same mechanism or target.

In summary, ABMA and DABMA appear as good leads for the development of new antiviral drugs against RABV infection targeting the late endosomal pathway. Further *in vivo* experiments are required to evaluate if they could participate, together with the anti-rabies serum, in a combined anti-RABV drug arsenal with synergistic effects at low concentrations, targeting different key steps of the RABV neuronal cycle.

**Fundings:**

The following programs contributed to fund the current research, both for material and fellowships: the joint ministerial program of R&D against CBRNE risks and Centre d'Energie Atomique (CEA - P/NRBC n°I1.1.8 "Large Spectrum Antivirals"); the European program ASKLEPIOS « Advanced Studies towards Knowledge on Lyssavirus Encephalitis Pathogenesis Improving Options for Survival » (FP7 - 602825 - Neglected infectious diseases of Central and Eastern Europe). In addition, the project benefited from the core facilities of the « Centre de Ressources et Recherches Technologiques » at the Institut Pasteur for imaging and bioinformatics.

**Conflicts of interest:**

None declared

**Acknowledgements :**

We deeply thank Dr Stefan Finke (Friedrich Loeffler Institute, Griefswald, Germany) for kindly providing a mouse MAb anti-M protein **;** Nathalie Aulner for her technical collaboration during the study.

| | ABMA | DABMA | ARBIDOL |
|---|---|---|---|
| $CC_{50}$ | >150µM | 41µM | 59 µM |
| $IC_{50}$ Pre-infection | 19.8µM | 7.8µM | 8.5µM |
| $IC_{50}$ Post-infection | >30µM | ~20 µM | >30µM |
| SI (Pre-incubation) | >7.5 | 5.4 | 6.9 |

**Table. 1. CC50, IC50, SI of ABMA, DABMA and Arbibol on RABV infection** The cytotoxicity (CC50) of each compound was evaluated by the ATP released in the cell supernatant after 24 h of contact with non infected BSR cells. The 50% inhibitory concentration (IC50) in pre or post-infection protocol was calculated using the Reed and Munch method. The Selectivity Index (SI) was only measured on the pre-infection protocol which was found more effective.

| Virus | SNPs | Depth | Freq% | (protein) AA |
|---|---|---|---|---|
| PV genbank VS PV input | 295 G-A | | | |
| | 2763 G-A | | | |
| | 2934 A-G | | | |
| | 3848 T-G | | | (G) D177L |
| | 4050 A-C | | | (G) G245L |
| | 4067 A-C | | | (G) S255A |
| | 4098 G-T | | | |
| | 4280 T-C | | | |
| | 4956 +1G | | | |
| | 5155 T-C | | | |
| | 6034 G-A | | | (L) N206D |
| | 7587 G-A | | | (L) V724L |
| | 8890 -1G | | | (L) C1128L |
| | 8902 +1C | | | |
| PV input VS PV 16 passages | | | | |
| | 5758 C-G | 8329 | 26 | |
| | 10265 A-G | 8159 | 22 | |
| | 10560 A-G | 8340 | 25 | |
| PV input VS PV Ribavirin 16 passages | | | | |
| | 2451 +A | 16264 | 16 | |
| | 8357 C-T | 35952 | 14 | |
| | 8809 T-C | 17655 | 14 | (L) S1128L |
| | 11162 T-C | | | |
| PV input VS PV ABMA 16 passages | | | | |
| | 2627 A-G | 15311 | 22 | (M) L43Q |
| | 3556 G-A | 15848 | 57 | (G) I83V |
| | 4943 +1G | 11790 | 69 | |
| | 5758 G-T | 12248 | 20 | (L) S113I |
| | 5923 C-T | 12310 | 52 | (L) N169D |
| PV input VS PV DABMA 16 passages | | | | |
| | 2765 C-A | 11712 | 19 | |
| | 2827 A-C | 11347 | 26 | |
| | 2939 T-G | 11681 | 50 | (M) D147L |
| | 3460 T-G | 11807 | 23 | (G) V48G |
| | 3772 T-C | 11704 | 42 | (G) V152A |
| | 3942 G-A | 11213 | 23 | (G) D209N |
| | 3956 T-G | 11759 | 26 | (G) A213L |
| | 4060 A-G | 11759 | 45 | (G) G247E |
| | 9125 G-A | 26784 | 11 | |
| | 9387 C-T | 26641 | 39 | |

**Table. 2. Frequency, read depth and position for each mutation screened by Pacbio over ABMA, DABMA and Ribavirin selection pressure**. The genome positions of the mutated nucleotides are indicated. The position of each amino acid change and the corresponding protein are also indicated.

**Fig.1. Effect of ABMA, DABMA and Arbibol on RABV infection.** BSR cells were infected with RABV (20MOI) in presence of increasing concentration of ABMA, DABMA and Arbibol compounds. Two protocols were compared. Pre-infection : 2 h pre-incubation of cells with the compounds before infection. Compounds were maintained during the 24 h of infection. Post-infection : incubation of cells with the compounds 2 h post infection and the compounds maintained for 24 h. The antiviral effect of the compounds in (A) Pre- and (B) Post-infection conditions was measured as the % of infected cells assessed through imaging identification of Negri bodies in their cytoplasm. In addition the RABV released in the cell supernatant was evaluated (C) by titration of infectious particles on fresh BSR cells using the plaque forming foci method; (D) by the amount of the RABV genomic RNA measured by qPCR using the SyberGreen Technology. The F primer was first used to reverse transcribe the (-) strand RABV genome, then 40 cycles of qPCR used F and R primers. The experiment was performed two times with two replicates for each condition.

**Fig. 2. Antiviral effect of ABMA, DABMA, and Ribavirin on RABV transcription and replication** :
A RABV minireplicon was reconstituted in BHK-T7 cells co-transfected with a Bluescript plasmid encoding a RABV minigenome expressing the luciferase and pTM1 plasmids coding for N, P, L RABV proteins (NPLDI). ABMA, DABMA and Ribavirin (20µM) were incubated simultaneously with the transfected plasmids. NPDI is the negative control, missing the plasmid encoding the RABV L polymerase. The amount of luciferase released from the cells after 48 h was measured.

**Fig. 3. Effect of ABMA and DABMA on early steps of RABV entry**

BSR cells were treated for 30 min with cycloheximide (CHX) (10µg/mL) alone, CHX + ABMA (60 µM), CHX + DABMA (40 µM) or CHX + EGA (40 µM). Then RABV infection was performed at very high MOI (500). (A) Income M protein was visualized by immunofluorescence 4 h and 9 h post-infection using a specific monoclonal antibody (green). Nucleus are colored by Hoechst (blue). (B) To quantify the RABV entry 9 h post-infection, 5 fields of 100 cells were counted for each compound in two independent experiments. Cells with at least 5 RABV M protein inclusions were reported as positive.
BSR cells were treated with ABMA at 60 µM or DABMA at 30µM following the pre-infection scheme. 24 h after infection (C) cells were stained with a Rab7a specific rabbit polyclonal antibody (red) and a RABV glycoprotein mouse monoclonal antibody (green) while nuclei were colored by Hoechst (blue). The images were taken with a confocal microscope using an X63 oiled objective. Cell lysates were obtained and the amount of (D) Rab7a mRNA was measured by quantitative PCR relative to the housekeeping gene RLP18 : the F primer was first used to reverse transcribe the (-) strand RABV genome, then 40 cycles of SYBRgreen qPCR used F and R primers. The experiment was performed two times with two replicates for each condition.

**Fig. 4. Bliss synergy/antagonism of pairwise combinations between ABMA, DABMA and Arbidol on RABV infection.**

Pairwise combinations of compounds at different concentrations were performed following the 2 h pre-incubation protocol and the antiviral effect was evaluated 24h post infection by imaging the Negri bodies in the cytoplasm of infected cells. (A) The raw data presented in the table were fit in a three dimensional matrix and the synergy (in blue) or antagonism (in red) between the couples of drugs was calculated by the software combenefit using Bliss

Independence Model formula of Synergy. (B) The graphs represent the antiviral effect of examples of combined compounds at the concentrations where they are the most synergetic.

**Fig. 5. Emergence of mutant selection of PV RABV in presence of drug pressure:** (A)

BSR cells were passaged 16 times without drugs or in the presence of increasing concentrations of Ribavirin, ABMA or DABMA at each passage (at 5, 6, 8, 10, 12, 13 (2 passages), 14 (2 passages), 15, 17, 18, 19, 20, 21 up to 22 µM). Neo-RABV produced at each passage were used to infect the next passage pre- treated with the increased concentration of drug (B) Schematic representation of mutations selected by long read sequencing technique (Pacbio). In blue are the synonymous mutations (genome position indicated). In red are the non-synonymous mutations (genome position indicated) and the corresponding amino acid change (protein position indicated). Table 3 indicates the frequency, read depth and position for each mutation

A

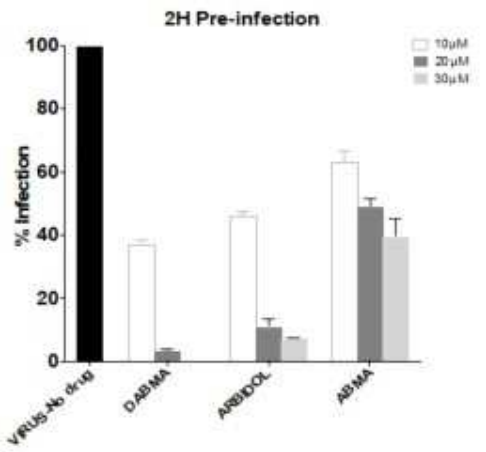
2H Pre-infection
% Infection
100
80
60
40
20
0
10μM
20μM
30μM
VIRUS-No drug
DABMA
ARBIDOL
ABMA

B

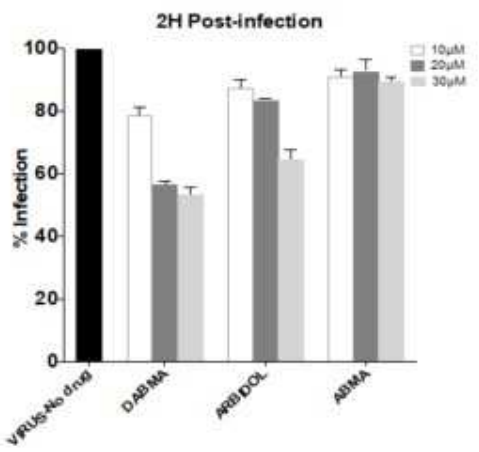
2H Post-infection
% Infection
100
80
60
40
20
0
10μM
20μM
30μM
VIRUS-No drug
DABMA
ARBIDOL
ABMA

C

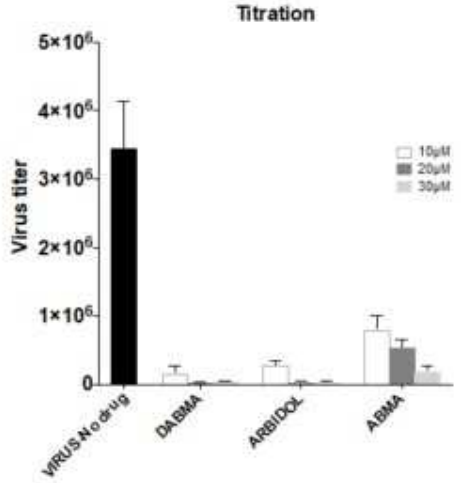
Titration
Virus titer
5×10⁶
4×10⁶
3×10⁶
2×10⁶
1×10⁶
0
10μM
20μM
30μM
VIRUS-No drug
DABMA
ARBIDOL
ABMA

D

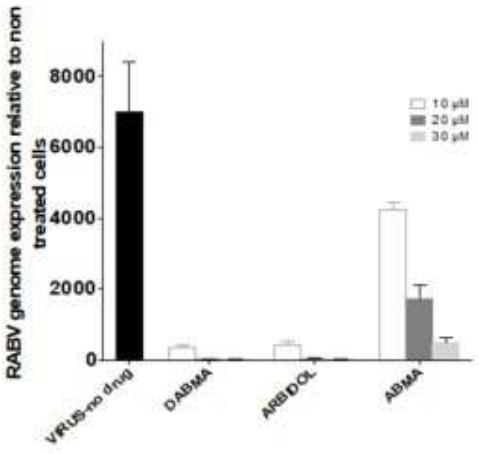
RABV genome expression relative to non treated cells
8000
6000
4000
2000
0
10 μM
20 μM
30 μM
VIRUS-no drug
DABMA
ARBIDOL
ABMA

**Fig.1.**

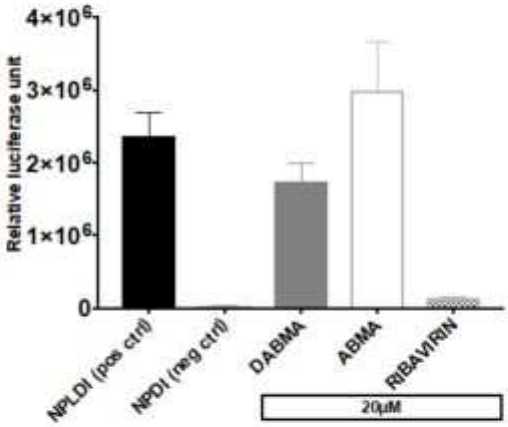
4×10^6
3×10^6
2×10^6
1×10^6
0
Relative luciferase unit
NPLDI (pos ctrl)
NPDI (neg ctrl)
DABMA
ABMA
RIBAVIRIN
20μM

**Fig. 2.**

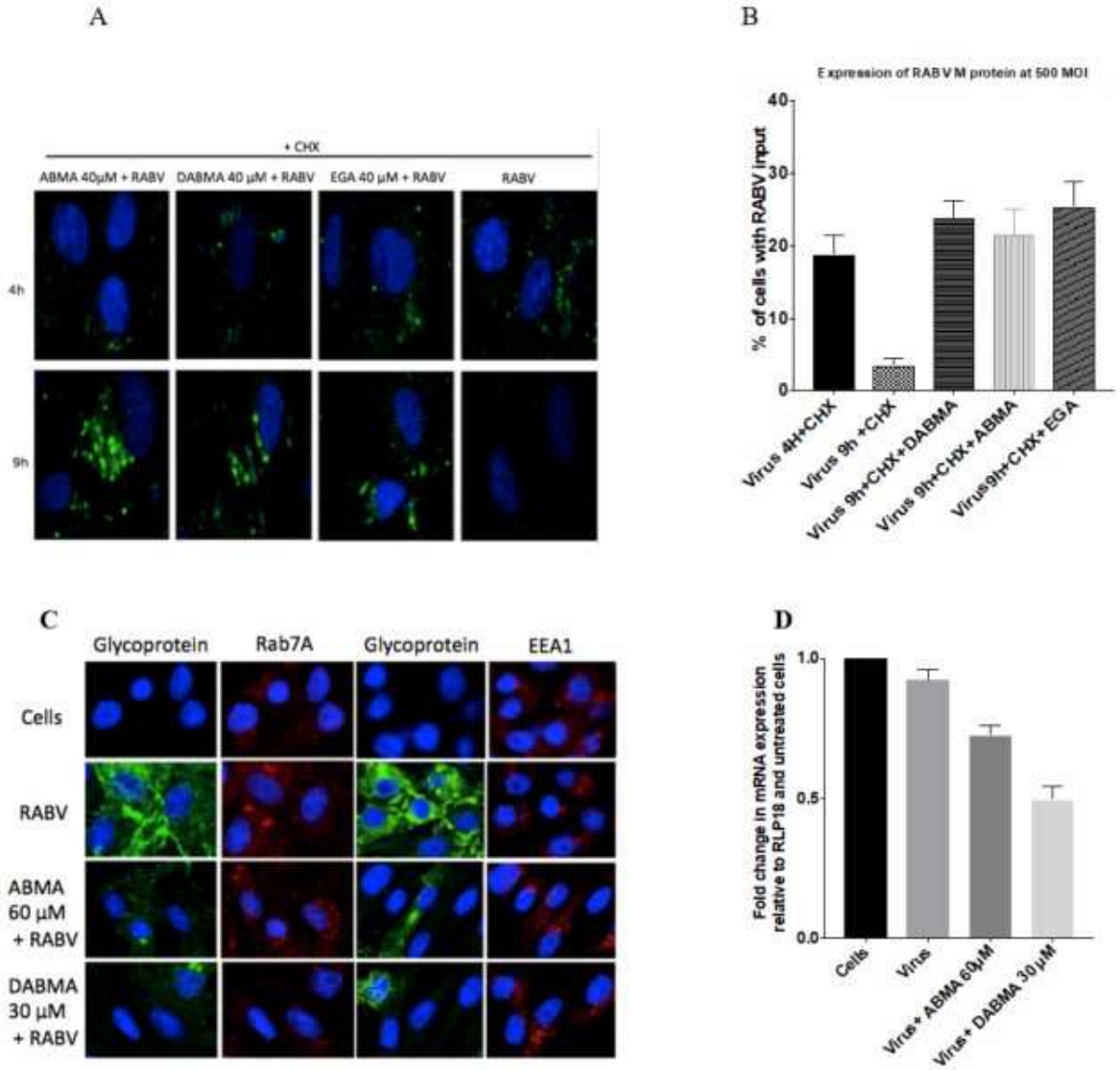
A
+ CHX
ABMA 40μM + RABV
DABMA 40 μM + RABV
EGA 40 μM + RABV
RABV
4h
9h
B
Expression of RABV M protein at 500 MOI
% of cells with RABV input
40
30
20
10
0
Virus 4H+CHX
Virus 9h +CHX
Virus 9h+CHX+DABMA
Virus 9h+CHX+ABMA
Virus 9h+CHX+EGA
C
Glycoprotein
Rab7A
Glycoprotein
EEA1
Cells
RABV
ABMA 60 μM + RABV
DABMA 30 μM + RABV
D
Fold change in mRNA expression relative to RLP18 and untreated cells
1.0
0.5
0.0
Cells
Virus
Virus + ABMA 60μM
Virus + DABMA 30 μM

**Fig. 3.**

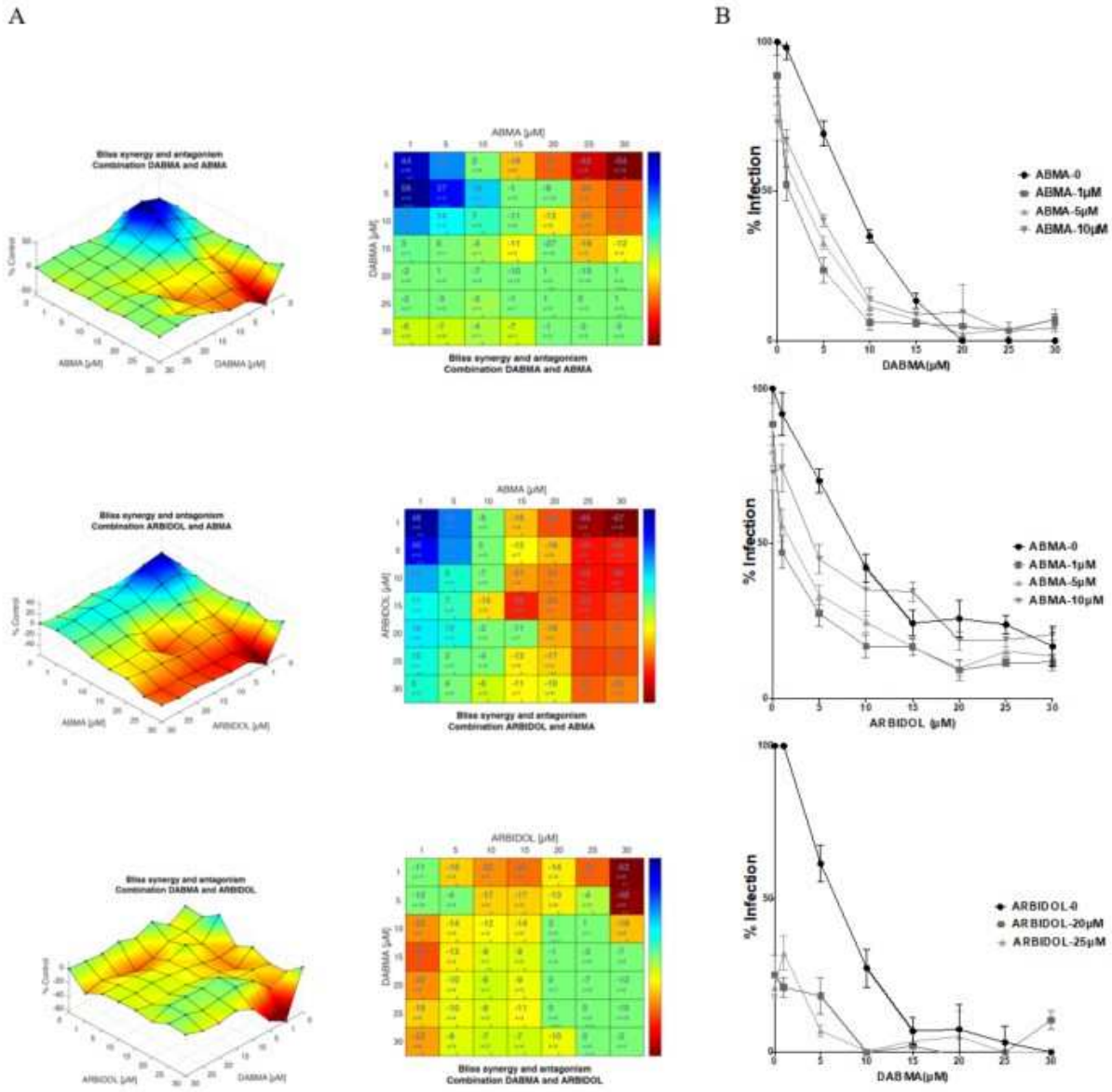
A
B
Bliss synergy and antagonism
Combination DABMA and ABMA
ABMA (μM)
DABMA (μM)
Bliss synergy and antagonism
Combination ARBIDOL and ABMA
ARBIDOL (μM)
Bliss synergy and antagonism
Combination DABMA and ARBIDOL
% Infection
DABMA(μM)
ABMA-0
ABMA-1μM
ABMA-5μM
ABMA-10μM
ARBIDOL (μM)
ARBIDOL-0
ARBIDOL-20μM
ARBIDOL-25μM

**Fig. 4.**

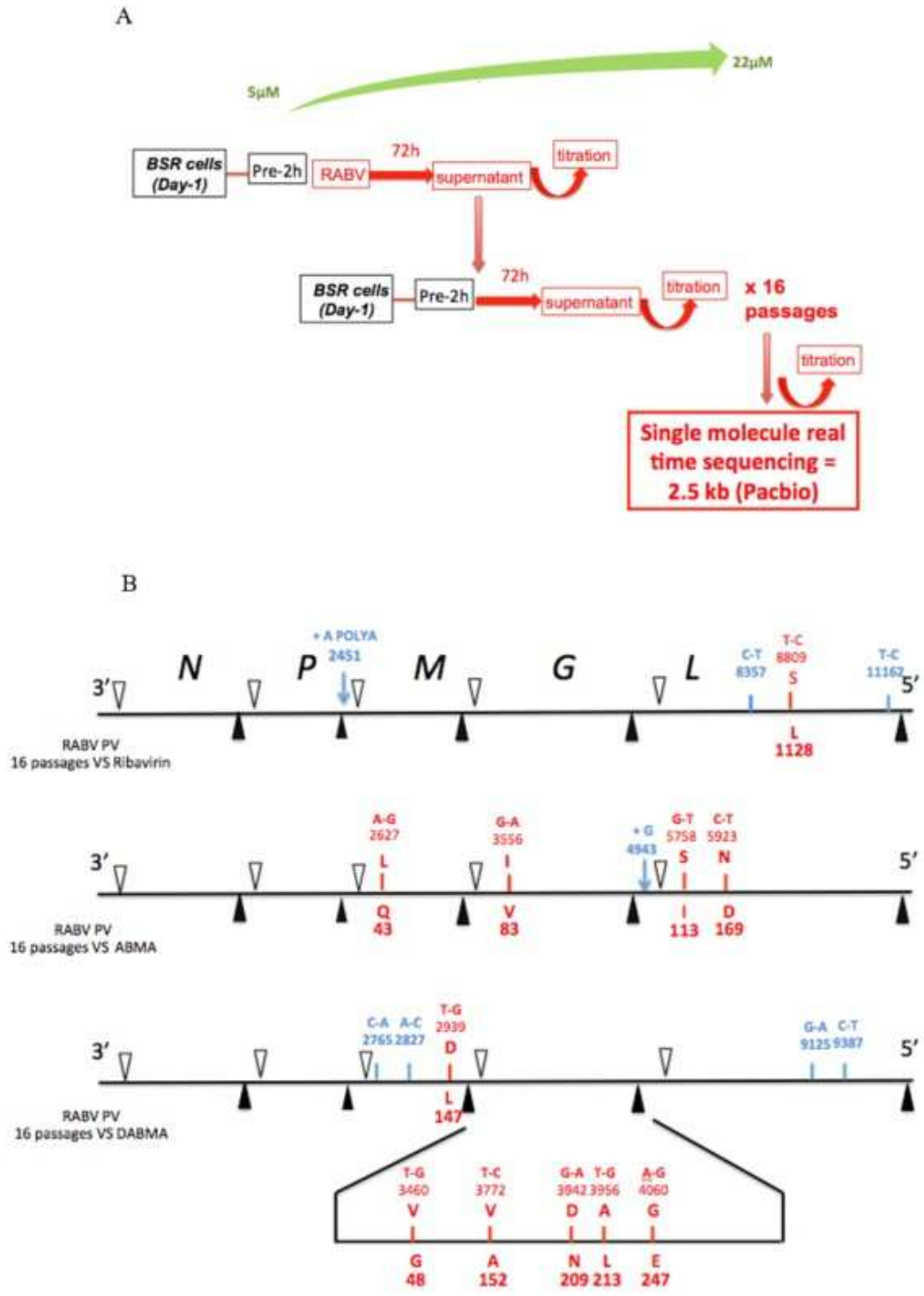
A
5µM
22µM
BSR cells (Day-1)
Pre-2h
RABV
72h
supernatant
titration
BSR cells (Day-1)
Pre-2h
72h
supernatant
titration
x 16 passages
titration
Single molecule real time sequencing = 2.5 kb (Pacbio)
B
3'
N
P
M
G
L
5'
+ A POLYA 2451
C-T 8357
T-C 8809
S
T-C 11162
L 1128
RABV PV 16 passages VS Ribavirin
A-G 2627
L
G-A 3556
I
+ G 4943
G-T 5758
C-T 5923
S
N
Q 43
V 83
I 113
D 169
RABV PV 16 passages VS ABMA
C-A 2765
A-C 2827
T-G 2939
D
G-A 9125
C-T 9387
L 147
RABV PV 16 passages VS DABMA
T-G 3460
V
T-C 3772
V
G-A 3942
T-G 3956
A
A-G 4060
G
G 48
A 152
N 209
L 213
E 247

**Fig. 5.**

**References :**

Arch Virol 164, 1967-1980.https://www.ncbi.nlm.nih.gov/pubmed/31089958.

Aramburo, A., Willoughby, R.E., Bollen, A.W., Glaser, C.A., Hsieh, C.J., Davis, S.L., Martin, K.W., Roy-Burman, A., 2011. Failure of the Milwaukee protocol in a child with rabies. Clin Infect Dis 53, 572-574. https://www.ncbi.nlm.nih.gov/pubmed/21865193.

Banyard, A.C., Mansfield, K.L., Wu, G., Selden, D., Thorne, L., Birch, C., Koraka, P., Osterhaus, A., Fooks, A.R., 2019. Re-evaluating the effect of Favipiravir treatment on rabies virus infection. Vaccine 37, 4686-4693. https://www.ncbi.nlm.nih.gov/pubmed/29132993.

Baquero, E., Albertini, A.A., Raux, H., Abou-Hamdan, A., Boeri-Erba, E., Ouldali, M., Buonocore, L., Rose, J.K., Lepault, J., Bressanelli, S., Gaudin, Y., 2017. Structural intermediates in the fusion-associated transition of vesiculovirus glycoprotein. EMBO J 36, 679-692. https://www.ncbi.nlm.nih.gov/pubmed/28188244.

Bekerman, E., S. Einav.2015. Infectious disease. Combating emerging viral threats. Science 348(6232): 282-283. https://www.ncbi.nlm.nih.gov/pubmed/25883340.

Belot, L., Albertini, A., Gaudin, Y., 2019. Structural and cellular biology of rhabdovirus entry. Adv. Virus Res. 104, 147–183. https://doi.org/10.1016/bs.aivir.2019.05.003

Bliss, C.I., 1939. THE TOXICITY OF POISONS APPLIED JOINTLY1. Annals of Applied Biology 26, 585-615.
https://onlinelibrary.wiley.com/doi/abs/10.1111/j.1744-7348.1939.tb06990.x.

Boriskin, Y.S., Leneva, I.A., Pecheur, E.I., Polyak, S.J., 2008. Arbidol: a broad-spectrum antiviral compound that blocks viral fusion. Curr Med Chem 15, 997-1005. https://www.ncbi.nlm.nih.gov/pubmed/18393857.

Bussereau, F., Chermann, J.C., De Clercq, D., Hannoun, C., 1983. Search for compounds which have an inhibitory effect on rhabdovirus multiplication In Vitro. Annales de l'Institut Pasteur / Virologie 134, 127-134.
https://www.sciencedirect.com/science/article/pii/S0769261783800483.

Bussereau, F., Picard, M., Blancou, J., Sureau, P., 1988. Treatment of rabies in mice and foxes with antiviral compounds. Acta Virol 32, 33-49.
https://www.ncbi.nlm.nih.gov/pubmed/2897770.

Castel, G., Chteoui, M., Caignard, G., Prehaud, C., Mehouas, S., Real, E., Jallet, C., Jacob, Y., Ruigrok, R.W.H., Tordo, N., 2009. Peptides that mimic the amino-terminal end of the rabies virus phosphoprotein have antiviral activity. J. Virol. 83, 10808–10820. https://doi.org/10.1128/JVI.00977-09

Castel G., Ben-Mechlia, M., Jallet, C., Tordo, N. 2015. Development of Anti-Viral Approaches. In Current Laboratory Techniques in Rabies Diagnosis, Research and Prevention, Volume 2, (C. Rupprecht & T. Nagarajan Eds)
http://dx.doi.org/10.1016/B978-0-12-801919-1.00027-0.

Castellanos, J.E., Martinez-Gutierrez, M., Hurtado, H., Kassis, R., Bourhy, H., Acosta, O., Lafon, M., 2005. Studying neurotrophin antiviral effect on rabies-infected dorsal root ganglia cultures. J Neurovirol 11, 403-410. https://www.ncbi.nlm.nih.gov/pubmed/16162483.

Crosby, N., Deane, K.H., Clarke, C.E., 2003. Amantadine in Parkinson's disease. Cochrane Database Syst Rev, CD003468. https://www.ncbi.nlm.nih.gov/pubmed/12535476.

Dai, W., Wu, Y., Bi, J., Wang, S., Li, F., Kong, W., Barbier, J., Cintrat, J.C., Gao, F., Gillet, D., Su, W., Jiang, C., 2018. Antiviral Effects of ABMA against Herpes Simplex Virus Type 2 In Vitro and In Vivo. Viruses 10. https://www.ncbi.nlm.nih.gov/pubmed/29522484.

Davies, W.L., Grunert, R.R., Hoffmann, C.E., 1965. Influenza virus growth and antibody response in amantadine-treated mice. J Immunol 95, 1090-1094.
https://www.ncbi.nlm.nih.gov/pubmed/29522484.

Debing, Y.,Emerson, S. U., Wang, Y., Pan, Q., Balzarini, J.,Dallmeier, K., Neyts, J.2014. Ribavirin inhibits in vitro hepatitis E virus replication through depletion of cellular GTP pools and is moderately synergistic with alpha interferon. Antimicrob Agents Chemother 267-273.
https://www.ncbi.nlm.nih.gov/pubmed/24145541.

Delogu, I., Pastorino, B., Baronti, C., Nougairede, A., Bonnet, E., de Lamballerie, X., 2011. In vitro antiviral activity of arbidol against Chikungunya virus and characteristics of a selected resistant mutant. Antiviral Res 90, 99-107.
https://www.ncbi.nlm.nih.gov/pubmed/21440006.

Deng, H.Y., Luo, F., Shi, L.Q., Zhong, Q., Liu, Y.J., Yang, Z.Q., 2009. Efficacy of arbidol on lethal hantaan virus infections in suckling mice and in vitro. Acta Pharmacol Sin 30, 1015-1024. https://www.ncbi.nlm.nih.gov/pubmed/19575005.

Di Veroli, G.Y., Fornari, C., Wang, D., Mollard, S., Bramhall, J.L., Richards, F.M., Jodrell, D.I., 2016. Combenefit: an interactive platform for the analysis and visualization of drug combinations. Bioinformatics 32, 2866-2868.
https://www.ncbi.nlm.nih.gov/pubmed/27153664.

Eduati, F.,Doldan-Martelli, V., Klinger, B., Cokelaer, T., Sieber, A., Kogera, F., Dorel,M., Garnett, M.J.,Bluthgen, N.,Saez-Rodriguez, J.2013. Drug Resistance Mechanisms in Colorectal Cancer Dissected with Cell Type-Specific Dynamic Logic Models. Cancer Res 77(12): 3364-3375. https://www.ncbi.nlm.nih.gov/pubmed/28381545.

Fooks, A. R.,Cliquet, F.,Finke, S.,Freuling, C.,Hemachudha, T.,Mani, R. S.,Muller, T. Nadin-Davis, S.,Picard-Meyer, E.,Wilde, H.,Banyard, A.C.2017. Rabies. Nat Rev DisPrimers 3: 17091. https://www.ncbi.nlm.nih.gov/pubmed/29188797.

Fournier-Caruana, J., Poirier, B., Haond, G., Jallet, C., Fuchs, F., Tordo, N.,Perrin, p.2003. Inactivated rabies vaccine control and release: use of an ELISA method." Biologicals 31(1): 9-16. https://www.ncbi.nlm.nih.gov/pubmed/12623055.

Gerzon, K., Kau, D., 1967. The adamantyl group in medicinal agents. 3. Nucleoside 5'-adamantoates. The adamantoyl function as a protecting group. J Med Chem 10, 189-199. https://www.ncbi.nlm.nih.gov/pubmed/4167033.

Gillespie, E.J., Ho, C.L., Balaji, K., Clemens, D.L., Deng, G., Wang, Y.E., Elsaesser, H.J., Tamilselvam, B., Gargi, A., Dixon, S.D., France, B., Chamberlain, B.T., Blanke, S.R., Cheng, G., de la Torre, J.C., Brooks, D.G., Jung, M.E., Colicelli, J., Damoiseaux, R., Bradley, K.A., 2013. Selective inhibitor of endosomal trafficking pathways exploited by multiple toxins and viruses. Proc Natl Acad Sci U S A 110, E4904-4912. https://www.ncbi.nlm.nih.gov/pubmed/24191014.

Graci, Jason D., Cameron, Craig E. 2006. Mechanisms of action of ribavirin against distinct viruses. Rev Med Virol 16, 37-48. https://www.ncbi.nlm.nih.gov/pubmed/16287208.

Grunert, R.R., McGahen, J.W., Davies, W.L., 1965. The in Vivo Antiviral Activity of 1-Adamantanamine (Amantadine). I. Prophylactic and Therapeutic Activity against Influenza Viruses. Virology 26, 262-269. https://www.ncbi.nlm.nih.gov/pubmed/14323994.

Hadi, C.M., Goba, A., Khan, S.H., Bangura, J., Sankoh, M., Koroma, S., Juana, B., Bah, A., Coulibaly, M., Bausch, D.G., 2010. Ribavirin for Lassa fever postexposure prophylaxis. Emerg Infect Dis 16, 2009-2011. https://www.ncbi.nlm.nih.gov/pubmed/21122249.

Hampson, K., Coudeville, L., Lembo, T., Sambo, M., Kieffer, A., Attlan, M., Barrat, J., Blanton, J.D., Briggs, D.J., Cleaveland, S., Costa, P., Freuling, C.M., Hiby, E., Knopf, L., Leanes, F., Meslin, F.X., Metlin, A., Miranda, M.E., Muller, T., Nel, L.H., Recuenco, S., Rupprecht, C.E., Schumacher, C., Taylor, L., Vigilato, M.A., Zinsstag, J., Dushoff, J., Global Alliance for Rabies Control Partners for Rabies, P., 2015. Estimating the global burden of endemic canine rabies. PLoS Negl Trop Dis 9, e0003709. https://www.ncbi.nlm.nih.gov/pubmed/25881058.

Haviernik, J., Stefanik, M., Fojtikova, M., Kali, S., Tordo, N., Rudolf, I., Hubalek, Z., Eyer, L., Ruzek, D., 2018. Arbidol (Umifenovir): A Broad-Spectrum Antiviral Drug That Inhibits Medically Important Arthropod-Borne Flaviviruses. Viruses 10. https://www.ncbi.nlm.nih.gov/pubmed/29642580.

He, L., Kulesskiy, E., Saarela, J., Turunen, L., Wennerberg, K., Aittokallio, T., Tang, J., 2018. Methods for High-throughput Drug Combination Screening and Synergy Scoring. Methods Mol Biol 1711, 351-398. https://www.ncbi.nlm.nih.gov/pubmed/29344898.

Hemachudha, T., Sunsaneewitayakul, B., Desudchit, T., Suankratay, C., Sittipunt, C., Wacharapluesadee, S., Khawplod, P., Wilde, H., Jackson, A.C., 2006. Failure of therapeutic coma and ketamine for therapy of human rabies. J Neurovirol 12, 407-409. https://www.ncbi.nlm.nih.gov/pubmed/17065135.

Ho, M., Nash, C., Morgan, C.W., Armstrong, J.A., Carroll, R.G., Postic, B., 1974. Interferon administered in the cerebrospinal space and its effect on rabies in rabbits. Infect Immun 9, 286-293. https://www.ncbi.nlm.nih.gov/pubmed/4816460.

Jackson, A.C., 2013. Current and future approaches to the therapy of human rabies. Antiviral Res. 99, 61–67. https://doi.org/10.1016/j.antiviral.2013.01.003

Jallet, C., Jacob, Y., Bahloul, C., Drings, A., Desmezieres, E., Tordo, N., Perrin, P., 1999. Chimeric lyssavirus glycoproteins with increased immunological potential. J Virol 73, 225-233. https://www.ncbi.nlm.nih.gov/pubmed/9847325.

Jochmans, D., Neyts, J., 2019. The path towards effective antivirals against rabies. Vaccine 37, 4660–4662. https://doi.org/10.1016/j.vaccine.2017.12.051

Lentz, T.L., Burrage, T.G., Smith, A.L., Crick, J., Tignor, G.H., 1982. Is the acetylcholine receptor a rabies virus receptor? Science 215, 182-184. https://www.ncbi.nlm.nih.gov/pubmed/7053569.

Lentz, T.L., Fu, Y., Lewis, P., 1997. Rabies virus infection of IMR-32 human neuroblastoma cells and effect of neurochemical and other agents. Antiviral Res 35, 29-39. https://www.ncbi.nlm.nih.gov/pubmed/9224959.

Loewe, S., 1953. The problem of synergism and antagonism of combined drugs. Arzneimittelforschung 3, 285-290. https://www.ncbi.nlm.nih.gov/pubmed/13081480.

Manesh, A., Mani, R.S., Pichamuthu, K., Jagannati, M., Mathew, V., Karthik, R., Abraham, O.C., Chacko, G., Varghese, G.M., 2018. Case Report: Failure of Therapeutic Coma in Rabies Encephalitis. Am J Trop Med Hyg 98, 207-210. https://www.ncbi.nlm.nih.gov/pubmed/29141755.

Mechlia, M.B., Belaid, A., Castel, G., Jallet, C., Mansfield, K.L., Fooks, A.R., Hani, K., Tordo, N., 2019. Dermaseptins as potential antirabies compounds. Vaccine 37, 4694-4700. https://www.ncbi.nlm.nih.gov/pubmed/29439871.

Moriyama, K., Suzuki, T., Negishi, K., Graci, J.D., Thompson, C.N., Cameron, C.E., Watanabe, M., 2008. Effects of introduction of hydrophobic group on ribavirin base on mutation induction and anti-RNA viral activity. J Med Chem 51, 159-166. https://www.ncbi.nlm.nih.gov/pubmed/18067241.

Paeshuyse, J.,Dallmeier, K.,Neyts, J.2011.Ribavirin for the treatment of chronic hepatitis C virus infection: a review of the proposed mechanisms of action. Curr Opin Virol **1**(6) 590-598. https://www.ncbi.nlm.nih.gov/pubmed/22440916.

Pecheur, E.I., Borisevich, V., Halfmann, P., Morrey, J.D., Smee, D.F., Prichard, M., Mire, C.E., Kawaoka, Y., Geisbert, T.W., Polyak, S.J., 2016. The Synthetic Antiviral Drug Arbidol Inhibits Globally Prevalent Pathogenic Viruses. J Virol 90, 3086-3092. https://www.ncbi.nlm.nih.gov/pubmed/26739045.

Piccinotti, S., Kirchhausen, T., Whelan, S.P., 2013. Uptake of rabies virus into epithelial cells by clathrin-mediated endocytosis depends upon actin. J Virol 87, 11637-11647. https://www.ncbi.nlm.nih.gov/pubmed/23966407.

Postic, B., Fenje, P., 1971. Effect of administered interferon on rabies in rabbits. Appl Microbiol 22, 428-431. https://www.ncbi.nlm.nih.gov/pubmed/4330317.

Prehaud, C., Coulon, P., LaFay, F., Thiers, C., Flamand, A., 1988. Antigenic site II of the rabies virus glycoprotein: structure and role in viral virulence. J Virol 62, 1-7. https://www.ncbi.nlm.nih.gov/pubmed/2446011.

Rupprecht, C., Kuzmin, I., Meslin, F., 2017. Lyssaviruses and rabies: current conundrums, concerns, contradictions and controversies. F1000Res 6, 184. https://www.ncbi.nlm.nih.gov/pubmed/28299201.

Schnell, M.J., McGettigan, J.P., Wirblich, C., Papaneri, A., 2010. The cell biology of rabies virus: using stealth to reach the brain. Nat Rev Microbiol 8, 51-61. https://www.ncbi.nlm.nih.gov/pubmed/19946287.

Stechmann, B., Bai, S.-K., Gobbo, E., Lopez, R., Merer, G., Pinchard, S., Panigai, L., Tenza, D., Raposo, G., Beaumelle, B., Sauvaire, D., Gillet, D., Johannes, L., Barbier, J., 2010. Inhibition of retrograde transport protects mice from lethal ricin challenge. Cell 141, 231–242. https://doi.org/10.1016/j.cell.2010.01.043

Superti, F., Seganti, L., Pana, A., Orsi, N., 1985. Effect of amantadine on rhabdovirus infection. Drugs Exp Clin Res 11, 69-74. https://www.ncbi.nlm.nih.gov/pubmed/3013559.

Tang, J., Wennerberg,k., Aittokallio,T. 2015. What is synergy? The Saariselka agreement revisited. Front Pharmacol 6, 181. https://www.ncbi.nlm.nih.gov/pmc/articles/PMC4555011/.

Thoulouze, M.I., Lafage, M., Schachner, M., Hartmann, U., Cremer, H., Lafon, M., 1998. The neural cell adhesion molecule is a receptor for rabies virus. J Virol 72, 7181-7190. https://www.ncbi.nlm.nih.gov/pubmed/9696812.

Tordo, N., Poch, O., Ermine, A., Keith, G., Rougeon, F .1986. Walking along the rabies genome: is the large G-L intergenic region a remnant gene? Proc Natl Acad Sci U S A 83, 3914-3918. https://www.ncbi.nlm.nih.gov/pubmed/3459163.

Tordo, N., Poch, O., Ermine, A., Keith, G., Rougeon, F .1988. Completion of the rabies virus genome sequence determination: highly conserved domains among the L (polymerase) proteins of unsegmented negative-strand RNA viruses. Virology 165, 565-576. https://www.ncbi.nlm.nih.gov/pubmed/3407152.

Tsiang, H.; Superti, F., Ammonium chloride and chloroquine inhibit rabies infection in neuroblastoma cells. *Arch Virol* 1984;**81**:377-82.

Tsiang, H., Ceccaldi, P.E., Ermine, A., Lockhart, B., Guillemer, S., 1991. Inhibition of rabies virus infection in cultured rat cortical neurons by an N-methyl-D-aspartate noncompetitive antagonist, MK-801. Antimicrob Agents Chemother 35, 572-574. https://www.ncbi.nlm.nih.gov/pubmed/1674849.

Wanka, L., Iqbal, K., Schreiner, P.R., 2013. The lipophilic bullet hits the targets: medicinal chemistry of adamantane derivatives. Chem. Rev. 113, 3516–3604. https://doi.org/10.1021/cr100264t

WHO.2020. https://www.who.int/rabies/en/

Willoughby, R.E., Jr., Tieves, K.S., Hoffman, G.M., Ghanayem, N.S., Amlie-Lefond, C.M., Schwabe, M.J., Chusid, M.J., Rupprecht, C.E., 2005. Survival after treatment of rabies with induction of coma. N Engl J Med 352, 2508-2514. https://www.ncbi.nlm.nih.gov/pubmed/15958806.

Wu, Y., Boulogne, C., Carle, S., Podinovskaia, M., Barth, H., Spang, A., Cintrat, J.C., Gillet, D., Barbier, J., 2020. Regulation of endo-lysosomal pathway and autophagic flux by broad-spectrum antipathogen inhibitor ABMA. FEBS J. https://www.ncbi.nlm.nih.gov/pubmed/31901207.

Wu, Y., Pons, V., Goudet, A., Panigai, L., Fischer, A., Herweg, J.A., Kali, S., Davey, R.A., Laporte, J., Bouclier, C., Yousfi, R., Aubenque, C., Merer, G., Gobbo, E., Lopez, R., Gillet, C., Cojean, S., Popoff, M.R., Clayette, P., Le Grand, R., Boulogne, C., Tordo, N., Lemichez, E., Loiseau, P.M., Rudel, T., Sauvaire, D., Cintrat, J.C., Gillet, D., Barbier, J., 2017. ABMA,

a small molecule that inhibits intracellular toxins and pathogens by interfering with late endosomal compartments. Sci Rep 7, 15567.
https://www.ncbi.nlm.nih.gov/pubmed/29138439
Wu, Y., Pons, V., Noel, R., Kali, S., Shtanko, O., Davey, R.A., Popoff, M.R., Tordo, N., Gillet, D., Cintrat, J.C., Barbier, J., 2019. DABMA: A Derivative of ABMA with Improved Broad-Spectrum Inhibitory Activity of Toxins and Viruses. ACS Med Chem Lett 10, 1140-1147. https://www.ncbi.nlm.nih.gov/pubmed/31413797.